Altitude compensating ringed nozzle

A. Jraisheh, J. Chutia, A. Benidar, V. Kulkarni

Altitude Compensating Ringed Nozzle

Ali Jraisheh[a,b], Jubajyoti Chutia[a], Abdessamad Benidar[c], Vinayak Kulkarni[a]

[a]*Department of Mechanical Engineering, Indian Institute of Technology Guwahati, 781039, Assam, India*
[b]*Department of Mechanical Engineering, Damascus University, Damascus, Syria*
[c]*Institut de Physique de Rennes, 35042, Rennes, France*

Abstract

The increased focus on supersonic and hypersonic flows necessitates methods to study such flows in laboratory-based facilities, thus motivating researchers to find effective, efficient, and affordable methods to produce them in laboratories. It is desirable for the rocket nozzles to operate efficiently at different altitudes, which made the Altitude Compensating Nozzles emerge as a solution. In this work, we propose a new design for such nozzles, namely, the ringed nozzle. The proposed nozzle consists of a stack of parallel rings that serve as a nozzle with bleeding slots. This design can be utilised to obtain different exit Mach numbers and attain the desired performance according to the pressure ratio, serving as an Altitude Compensating Nozzle. The stack of rings might be altered to tailor nozzle shape and area ratio corresponding to the nozzle requirement. The nozzle is analysed from an engineering perspective by comparing the thrust coefficient and specific impulse, and the numerical simulations show promising results.

Keywords: Supersonic Nozzle, Altitude Compensating Nozzle, Bleeding Slots

Abbreviations

ACN Altitude Compensating Nozzle
ASO Aerodynamic Shape Optimisation
AUSM Advection Upstream Splitting Method
CB Conventional Bell
CFD Computational Fluid Dynamics
C_t Thrust Coefficient
I_S Specific Impulse
LTE Local Thermal Equilibrium

MoC Method of Characteristics
NPR Nozzle Pressure Ratio

1. Introduction

The need for reliable and affordable means to produce a supersonic/hypersonic jet has rapidly increased with the evolution of space flights. The nozzle that produces such jets is the integral part of turbojet or rocket engine. But the high speed nozzles are also required for understanding chemical processes or for spectroscopic measurements. Freejet is even important in studying the gas condensation [1, 2, 3], understanding radioactive atoms [4] and non-Local Thermal Equilibrium (non-LTE) molecules spectroscopy [5]. The kinetics of gas phase reaction at very low temperature for astrophysical applications of neutral [6] or charged [7] species are studied as well using either continuous [8] or pulsed [9, 10, 11] operating de Laval nozzles. All these applications demand an optimum nozzle that is capable of emitting a uniform jet. Therefore, many researchers focused on designing an optimum nozzle.

1.1. Nozzle Shape Optimisation

According to the desired application, the nozzle profile can differ from symmetric shape which is used for rockets and wind tunnel experiments, to non-symmetric nozzle which can be found in optical sensors and optical windows [12]. The nozzle geometry also plays an important role in determining the jet penetration depth, and in the droplet formation and distribution in spray jets [13]. Kbab et al. [14] have used the method of characteristics (MoC) to design a dual-bell nozzle profile that operates ideally under two different pressure ratios without the need of mechanical activation. They used the transonic flow approaches to determine the line at which the supersonic calculations start. The base nozzle is designed with the (MoC) and the latter nozzle is constructed as a second-degree polynomial. Recently, Emelyanov et al. [15] have numerically calculated the forces exerted on such nozzles due to the movement of the extendable part. A previous study by Munday et al. [16] has shown that a conical nozzle differs from smoothly-contoured nozzle by two aspects. Firstly, they have a sharp throat which causes the formation of a shock wave within the nozzle, hence making it impossible to achieve a shock-free operation. Secondly, the continuously-diverging wall causes the flow to gain a certain radial velocity at the nozzle exit, i.e., the flow

would be directed outwards at the exit plane. Each of these two aspects creates a diamond shock, which introduces a double-diamond configuration within the jet, regardless of it being underexpanded, overexpanded, or ideally-expanded. Moreover, Perumal and Rathakrishnan [17] experimentally proved that, for circular jet, the length of supersonic jet core, or the inviscid core, is highly dependent on the exit pressure ratio (ratio of nozzle exit pressure to back pressure). Many applications [5, 18] require this supersonic core to be as uniform and long as possible, and therefore it becomes crucial to grasp the influence of other factors on the jet core, including the nozzle wall shape. Rao [19] constructed the diverging part of a nozzle contour, for optimum thrust performance, by integrating an arc immediately downstream the throat with a quadratic Bézier curve to form a bell contoured nozzle. Similar methodology was found suitable to obtain an optimised Scramjet nozzle [20] for a fixed combustor outlet. Recently, Brahmachary and Ogawa [21] used a multi-point multi-objective optimisation technique to address the impact of geometrical parameters on the intake performance of a Busemann-based Scramjet, in the sense of compression efficiency and drag reduction. Further, Aerodynamic Shape Optimisation (ASO) can also be a useful tool to obtain a nozzle geometry that provides both efficient propulsion and low-noise performance. It is evident that CFD-based ASO can be computationally cumbersome [22], and therefore, before feeding the problem to a more sophisticated solver, it is more efficient to study the influencing factors using a low-fidelity approach. Jraisheh et al. [23] have developed a low-fidelity solver based on simple gas dynamics relations to construct a supersonic nozzle wall shape with restricted angle of divergence. The nozzle is capable of producing a uniform flow at the exit and for several diameter downstream. Moreover, Heath et al. [24] used a one-dimensional gas dynamics solver, along with the method of characteristics, to build a nozzle wall geometry, and then introduced a plug to reduce the noise. Here, the objective was to reduce the pressure disturbance at and downstream of the nozzle exit which would in turn reduce the noise, and this reduction is important for supersonic flight approval. Atkinson and Smith [25] adopted the method of characteristics to develop the diverging part of a supersonic nozzle wall. Since this method does not account for the boundary layer which has the major viscous effects and heat transfer, they added the displacement thickness, δ^*, to the resulting contour to include the viscous region in the nozzle wall shape. Davidenko et al. [26] considered a direct optimisation for the maximum thrust nozzle shape with a center body for different nozzle lengths and diameters. Variation of the diameter of center body was found to change the thrust for both inviscid as well as viscous wall boundary conditions. Mason and Broadhurst [27] employed Monte Carlo based mathematical model to

solve the problem of gas misalignment while using multiple nozzles on a single rocket motor, since the thrust alignment is not an issue in case of a single nozzle. This approach is based on a series of random selections that start from pre-defined probability distribution.

1.2. The Concept of Altitude Compensation

Among the available choices, Conventional Bell (CB) nozzle is one of the widely-used nozzles for rocket flights, although its efficiency is widely dependent on the back pressure. The rocket nozzle, generally, is designed to perform between a fixed chamber pressure and a varying back pressure, and this would alter the efficiency of the nozzle while operating at off-design conditions. Hence, Altitude Compensating Nozzles (ACN) are introduced [28, 29], including the dual-bell nozzle [30], cooled dual-bell nozzle [31, 32], and the fixed geometry nozzle, that support a controlled separation from the nozzle wall, at a desired "effective" area ratio. Dual-bell ACN tackles the problem of varying Nozzle Pressure Ratio (NPR), whether the two bells are fixed or the second bell forms a nozzle skirt for high altitude conditions. This nozzle utilises the first bell when the pressure ratio is low, i.e, at low altitudes, and includes the second bell when the back pressure drops, leading to increase in pressure ratio, at high altitudes, so as to maintain the ideal expansion at all operating conditions. That is, the rocket nozzle efficiency is considered to be higher when all the streamlines are normal to the exit cross-section [33], and this condition corresponds to the ideal expansion of the nozzle. The operation condition of a dual-bell nozzle is sketched in the schematic Fig. 1. Moreover, aerospike-shaped pintle nozzle Ha and Kim [34] is proven to be a viable option for varying thrust as the variation of throat area alters the performance of the solid rocket motor.

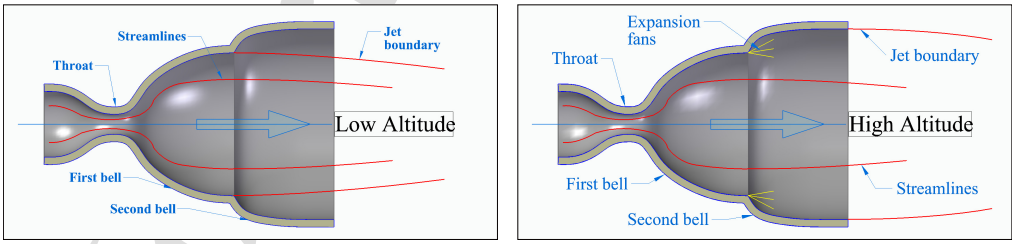

(a) (b)

Figure 1: A schematic figure of the operation of a dual-bell nozzle: (a) Low altitude operation and (b) High altitude operation.

Furthermore, bleeding slots in supersonic flow ducts have been used to reduce the boundary layer separation from adverse effects of shock wave-boundary layer interaction. The bleeding holes introduce different effects on the duct flow according to their width, length and angle [35]. Researchers have proved that, introducing bleed slots in the supersonic inlets can suppress the shock-induced separation resulting from the interaction between turbulent boundary layer and normal shock [36]. It is evident that the presence of multiple bleed slots could "improve" the boundary layer by drawing off the low momentum part of the fluid, which in turn increases the the average kinetic energy carried by the boundary layer, and hence making it less vulnerable for separation [37]. Moreover, as it is desired to control the growth of boundary layer in the inlets [38], it is also important to mitigate its effect at the outlet or within the nozzle. Further, Weiss and Olivier [39] concluded that, despite the loss in mass flow rate caused by the bleeding system, the static pressure gradient strengthens due to the bleeding. However, the total pressure recovery is less efficient in this system because of the mass loss.

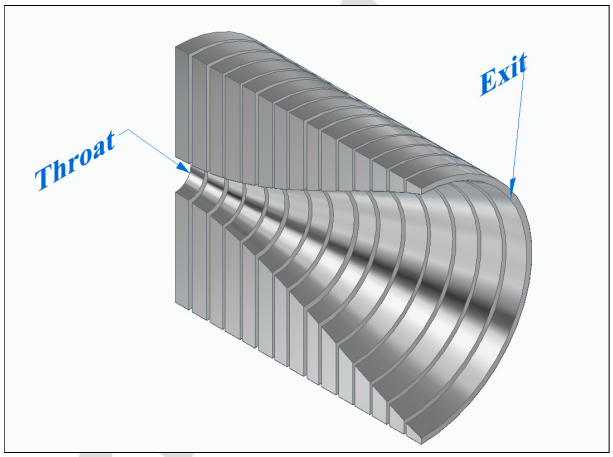

Figure 2: A 3*D* view of the ringed nozzle arrangement.

1.3. The Proposed Approach

It can be noticed from the literature that the nozzle shape optimisation is highly desirable in many engineering and scientific applications [23]. But, it must be noted that the design of optimum solid nozzle is based on fixed operating conditions and any change in these conditions would alter the nozzle performance. Hence, for getting the optimum performance, there is requirement of a separate solid nozzle for each nozzle operating condition. Besides, a nozzle that is designed for

a specific pressure ratio can only operate ideally at that pressure ratio. A rocket nozzle, for example, experiences a variety of back pressures from launching to exiting earth atmosphere. Moreover, a spectroscopic experiment may require different flow parameters, which necessitates different exit Mach number each time. These requirements demand supersonic nozzles with adjustable area ratio (mostly exit area), and that is why ACNs were adapted for many applications. The available ACNs have a few limitations like operating in a small range of pressure ratio (dual-bell nozzle operates optimally on two pressure ratios). Hence, it is proposed to apply the concept of multiple area ratios on a wider range, by introducing more than two stages of operation. Therefore, ringed nozzle would possibly solve the issue of varying back pressure due to variation in altitude and produce jets with varying parameters as per the laboratory requirements. A sectional $3D$ view of the suggested arrangement is shown in Fig. 2. Such arrangement is also effective for nozzle wall-based boundary layer control through suction of low momentum flow. It is believed that the ringed nozzle introduces different advantages to the jet, which correspond to the requirement of different applications. Various arrangements of the rings are possible by altering the gap width among them, which helps in controlling the boundary layer growth. Compensation for the change in the external pressure can also be obtained by re-arranging the existing rings to alter the nozzle area ratio, which is the leading parameter that corresponds to the pressure ratio. This can be done by adding or removing one ring or more at the nozzle exit, or can be achieved by fabricating the rings from flexible materials that allow area adjustment. Moreover, reduction of nozzle weight or less material requirement is an added advantage of the stacked-rings nozzle along with its adaptability for different operating conditions. In case of the spectroscopic studies, there is indeed a requirement of optimum nozzle for uniform flow at the exit along with a large inviscid core. Hence, initial objective of current study is to propose a novel ringed nozzle design or nozzle shape, for such applications [5, 6, 7, 8, 9, 10, 11], using steepest descent optimisation algorithm for a minimum exit radial velocity [23]. Such studies are desirable to reduce the number of nozzles required for each operating condition. Hence, the current approach is mainly proposed as a proof-of-concept, and to assist laboratory studies that demand such requirement. However, argon is prominently used in those investigations [5], therefore argon is used in the present studies as well. Thus, current proposition targets replacement of the rigid nozzle wall with a stack of rings to introduce flexibility in the design as to form different nozzle shapes. The proposed nozzle is designed through optimization process and tested using CFD to provide an insight on its utility. In this regard, section 2 explains the numerical methods and the computational domain, section

3 deals with the results obtained numerically using the in-house CFD solver, and section 4 summarizes the findings.

2. Methodology

2.1. Low-fidelity solver formation

The nozzle wall shape is obtained as per the low-fidelity flow solver [23], using a third order Bézier curve to represent the nozzle wall and the method of gradient steepest descent to minimise the radial velocity at the nozzle exit. After dividing the nozzle length into 100 divisions, the optimisation technique considers the dimensions of the nozzle (in this case, inlet diameter of 2 *mm*, exit diameter of 24 *mm* and a length of 30 *mm*), the total temperature (in this case $T_0 = 1300\ K$), and the gas properties (Argon) as inputs. Using the quasi one-dimensional gas dynamics relations, the solver calculates local Mach number, static temperature, and the speed of sound at each division. Having these values, first, total velocity is calculated and then the radial velocity is estimated using exit angle of divergence. To account for the growth of boundary layer, the value of radial velocity at the nozzle exit is set to approach a small value (5% of the total velocity). It may be noted that the boundary layer pushes the flow towards the axis (negative radial velocity) and cancels out the positive radial velocity obtained by the inviscid one-dimensional solver. The optimisation algorithm then finds the locus of the nozzle wall that corresponds to the minimum radial velocity (objective function) at the exit. As an additional constraint, a penalty function is added to the objective function as the initial angle of divergence. This penalty constraints the gas expansion within the nozzle, which extends the potential core further downstream. Further details pertaining to the optimization can be found in Jraisheh et al. [23].

2.2. Flow Solver formulation

Thus obtained coordinates of the nozzle wall are arranged to form stacked coaxial rings in a computational domain for CFD solver to get the detailed flow features. The flow solver accounts for Navier-Stokes equations in their axisymmetric form, considering laminar compressible flow and ideal gas. While high-speed flows might be asymmetrical as they evolve with time, the final steady-state solution is proven to be axisymmetric for axisymmetric nozzles [40, 41]. Therefore, the axisymmetric form of governing equations is employed. Further, the shock waves and jet dynamics are mostly inviscid in nature, but the evolution of boundary layer in such high-speed flows is significant. Hence, Navier-Stokes

equations are used with laminar flow assumption, which is valid for short nozzles used in laboratories, and the gas can be considered ideal under the chosen operating temperature. These equations are solved along with the equation of state to obtain the flow field variables, i.e., ρ, u, v, E, P, T. The convective fluxes are obtained using the advection upstream splitting method (AUSM) with second order accuracy, while the viscous fluxes are obtained using central differencing, with the viscosity dependence on temperature evaluated using two-terms Sutherland's law. The solution is considered to be converged when the normalised residue attains 10^{-6}. This solver has been considered for other applications as well, and the details of estimation of temporal accumulated error are available in the literature [42, 43, 44, 45, 46]. Moreover, the method to estimate the error accumulation in aerodynamic simulations is described in [47, 48]. Here, CFD simulations provide details of flow field which are essential to analyse the nozzle flow, especially for current studies which involve ringed nozzle. Such simulations are performed for a conventional solid nozzle and are validated by experiment [23], and therefore they are performed for the ringed nozzle in order to compare its performances with the conventional nozzle.

2.3. Computational Domain and Boundary Conditions

As the supersonic/hypersonic nozzle flow is highly sensitive to the domain, it requires to extend the dimensions of the domain so that the boundary conditions do not affect the internal flow field, and to prevent the interaction between boundaries [49]. Thus, the length of the domain is kept as 300 throat diameters, and its height as 150 throat diameters. This domain includes the supersonic part of the nozzle, gaps between the rings and nozzle outlet. Hence, the domain inlet is set for sonic conditions. The nozzle wall and rings are treated as adiabatic walls. It is to be mentioned that the gap height matches the domain height downstream of the nozzle exit, for the sake of consistency. The subsonic part of the nozzle does not have a significant impact on the jet, and the flow can be treated as uniform at the throat, assuming a contoured converging part. This assumption is already addressed and justified [50]. The computational domain is initialised with the outlet pressure and temperature, and is illustrated in Fig. 3 along with the boundary conditions. The mesh lines are clustered towards the nozzle interior and near-field to capture the flow accurately. The method of meshing takes care of the gaps between the rings which are part of this computational domain, hence the same governing equations are solved here as well with the same boundary conditions. The initial mesh has $59,400$ nodes which are then enhanced up to $81,000$. A further enhancement in the mesh, up to $141,300$ nodes shows a similar solution as

that of the previous mesh. Hence, the solution is found to be independent of the mesh at 81,000 nodes. Figure 4 illustrates the ratio of jet pressure at the axis to the back pressure. One can infer from this figure that the flow at the axis expands rapidly from the inlet of the domain (throat) until its pressure approaches the back pressure (represented here by $P_{jet}/P_b = 1.0$).

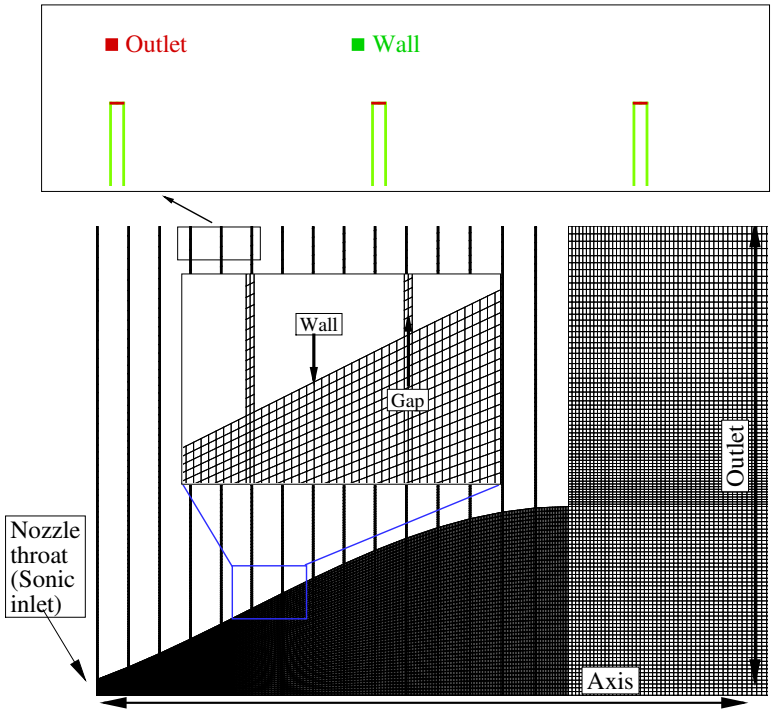

Figure 3: Domain and mesh used for the simulations.

3. Results

Supersonic nozzle flow has a complicated jet structure, having boundary layer, expansion waves downstream the throat, extended shear layer downstream the nozzle exit, and the point of jet reflection. These flow features get altered with the boundary conditions and nozzle geometry. Nevertheless, typical features of the underexpanded jet are illustrated in the numerical schlieren image (Fig. 5) obtained from the current CFD simulation for a typical governing nozzle pressure ratio of 2055 and a conventional conical nozzle. The flow features depicted in this

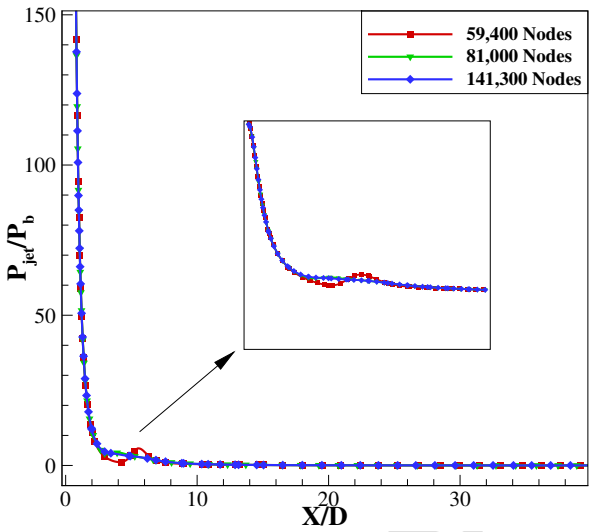

Figure 4: Axial distribution of the jet pressure ratio for three different meshes.

figure would be referred in the analysis.

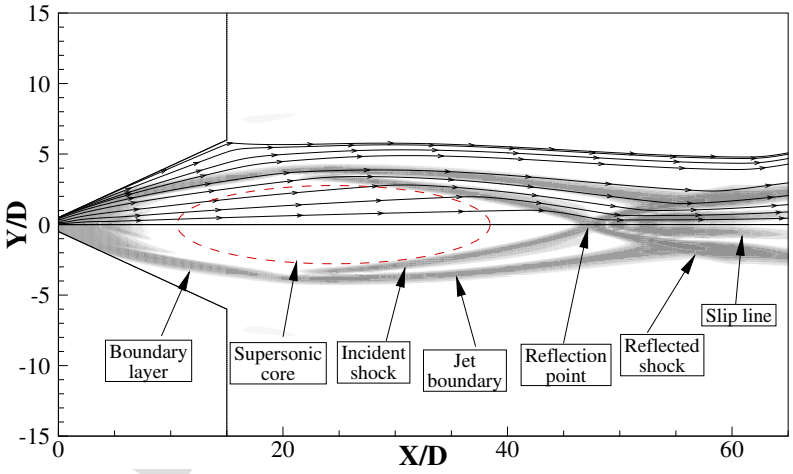

Figure 5: Supersonic jet components.

The usability of the proposed ringed nozzle is initially addressed numerically, considering Argon ($\gamma = 1.67$ and $R = 208\ J/kgK$) to be the working fluid for its significance in spectroscopic applications. The nozzle is designed accord-

ingly with a throat diameter of 2.0 *mm*, exit diameter of 24.0 *mm* and a length of 30.0 *mm*, along with 1300 *K* total temperature. The nozzle pressure ratio, NPR, is set as 2055, which corresponds to exit pressure ratio of 1000, considering Argon properties.

3.1. Conical ringed nozzle

The conical nozzle is capable of producing a supersonic jet with almost the desired Mach number. However, the produced jet at the nozzle exit and downstream has a certain non-uniform radial distribution for Mach number and other jet properties, like density and temperature. This discrepancy is caused by the growth of boundary layer. Therefore, the design of optimised contoured nozzle tackles these challenges. Moreover, the gaps between the rings allow a gas loss from the flow, and that has an influence on the flow properties within and downstream the nozzle. Hence, numerical schlieren images are used to illustrate the flow field.

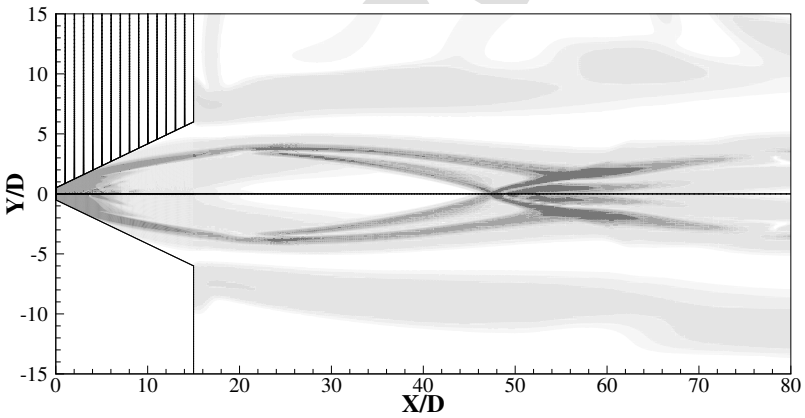

Figure 6: Numerical schlieren image for conical nozzle (bottom) and conical ringed-nozzle (top).

Initial simulation is performed to compare the flow through ringed conical nozzle and the classical conical nozzle. Here, the gap between the rings is considered to be 0.1 *mm*, which corresponds to 0.05 throat diameter. Figure 6 shows a comparison between the numerical schlieren contours for the regular conical nozzle and the ringed conical nozzle with the same above-mentioned dimensions. One can notice from the figure that the jet is not remarkably altered by replacing the regular nozzle with rings. This can be attributed to the small amount of mass

that bleeds through the gaps between the rings. Moreover, the conical nozzle has a constant slope, which may not conform to the jet boundaries within the nozzle. Therefore, the flow is merely attached to the nozzle wall as shown in the figure, and hence the mass loss is minimum. This effect emphasises the importance of contoured nozzle. The total pressure probed on the axis at the exit plane is found to drop by 0.64% when using the above-mentioned rings.

3.2. Contoured ringed nozzle

Efforts are then extended to design a contoured nozzle using the method discussed earlier for the same constraints and conditions. Further, the contoured nozzle is also replaced with stacked rings, and few simulations are performed on the resulting domain with different gap widths. Figure 7 shows the effect of altering the bleeding gaps between the stacked rings. Relatively large gap leads to more mass loss which decreases the jet mass flow rate. Therefore, as the gap decreases, the jet attains higher mass flow rate, and higher local pressure as a result. Thus the supersonic core length is approximately 27 throat diameter downstream for a gap width of $0.3D$, and it extends to $29D$ and $31D$ for a gap width of $0.15D$ and $0.05D$, respectively. This is also reflected in the axial pressure distribution in Fig. 8.

Moreover, it is evident from Fig. 7c that, the supersonic core of the jet, for a small gap width, almost attains the location of the reflection point for the conventional contoured nozzle. This shows that minimizing the gap width decreases the lost mass flow through the bleeding slots and makes it approach the performance of a conventional nozzle. Thus, the expansion trend, represented by axial pressure distribution, has to be thoroughly studied to discriminate the influence of each set of rings on the resulting jet. Figure 8 illustrates the axial pressure distribution, from the nozzle throat up to $50D$ downstream, for the conventional contoured nozzle compared to the ringed nozzles with different gap width.

It is also seen in Fig. 8 that the conventional nozzle and the ringed nozzle with the smallest gap width ($0.05D$) have matching axial reflecting points, around $31D$ downstream the nozzle exit plane, compared to nozzles with wider gaps, that have reflection points at $29D$ and $27D$ downstream for a gap width of $0.15D$ and $0.3D$, respectively. This is imputed to the higher mass flow rate in case of conventional nozzle, and the almost negligible mass loss in the narrow gap, $0.05D$. The pressure distribution is also seen to be disturbed within the nozzle in the initial phase of

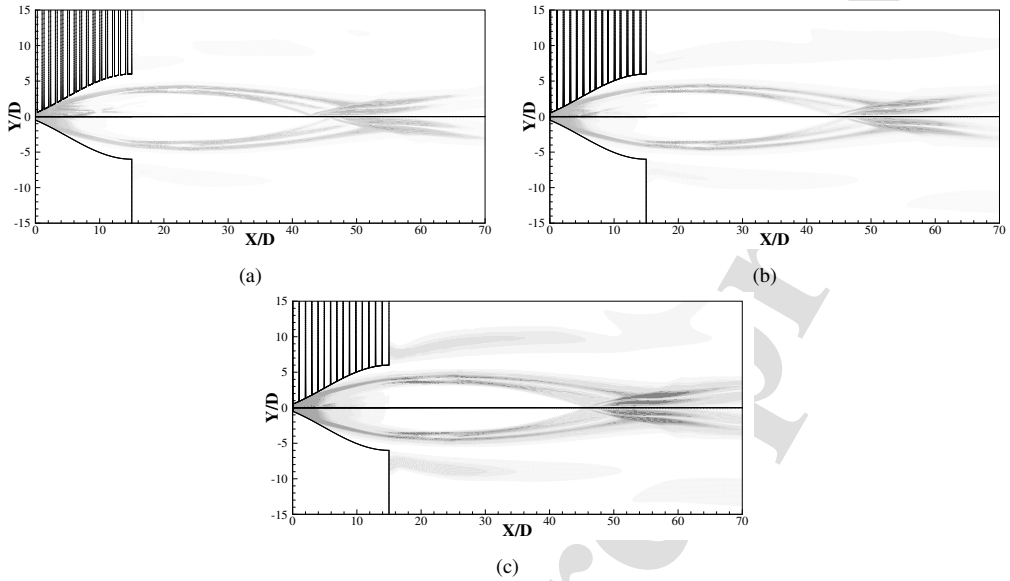

Figure 7: Numerical schlieren images of a conventional nozzle versus ringed nozzles with different gap widths: (a) Gap width =0.3D, (b) Gap width =0.15D and (c) Gap width =0.05D

expansion while using the stack of rings. Nonetheless, it is seen to be smooth for the conventional nozzle. This is due to the sharp-edged ring that impacts the flow and causes what appears to be a slight pressure increment for wider gaps. However, this effect is not noticed in the flow within the conventional nozzle, and it is nearly not visible for ringed nozzle with gap width 0.05D, and it is seen to be more impactful as the gap width increases, because the flow expands over a longer distance and increases its Mach number before impinging on the sharp edge of the first ring. Hence, the gap width is recommended to be as narrow as possible to imitate the performance of a conventional nozzle and avoid the formation of a weak shock within the nozzle. Nevertheless, this weak shock gets weaker and vanishes as it propagates within the nozzle, as observed in the schlieren images in Fig. 7.

3.3. Performance analysis

Although the bleeding slots take away the low-momentum part of the flow, they deprive the flow from certain energy content along with the lost mass flow. Therefore, as an indicator for potential, the total pressure ratio, PR_0, which is the ratio between the total pressure at the nozzle exit, $P_{0,e}$, to the total pressure at the nozzle inlet (stagnation pressure), P_0, is calculated as per Eq. 1 and plotted in Fig.

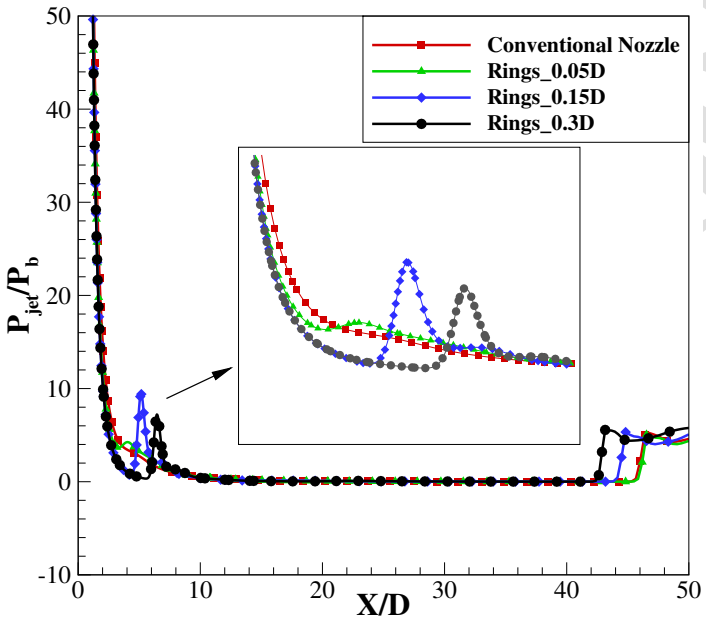

Figure 8: Axial pressure distribution for the conventional and ringed nozzles.

9.

$$PR_0 = \frac{P_{0,e}}{P_0} \tag{1}$$

where, $P_{0,e}$ is the total pressure at the intersection point of nozzle axis and nozzle exit plane for the conventional contoured nozzle and the ringed nozzles with a certain gap width, $0.05D$, $0.15D$ and $0.3D$.

It can be clearly seen from Fig. 9 that total pressure decreases when the rings are introduced, and decreases further as the gap width increases. The total pressure ratio attains values of 75%, 80% and 98% for gap width of $0.3D$, $0.15D$ and $0.05D$, respectively. Further, the flow seems to keep more than 99% of its total pressure as it expands through the conventional nozzle, and thus indicates an isentropic expansion throughout the chosen nozzle. Therefore, the presence of bleeding slots at the nozzle wall eliminates a certain amount of the flow potential, and this effect can be mitigated by narrowing the gap width between the stacked rings. To analyse the nozzle performance, the thrust coefficient and specific impulse, for the contoured nozzle and subsequent ringed nozzle, are calculated as

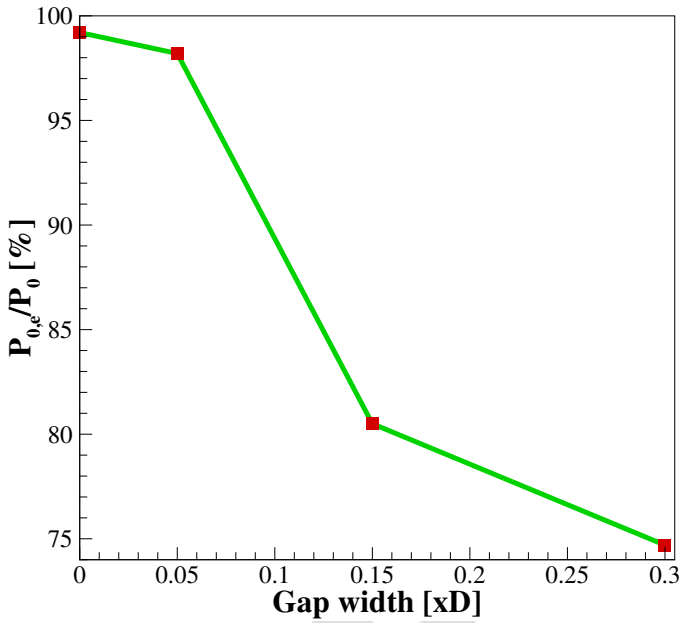

Figure 9: Ratio of total pressure at the nozzle exit plane vs. the gap width

follows:
The thrust is calculated as,

$$T = m^*.V_{exit} + (P_e - P_b)A_e \tag{2}$$

where m^* is the mass flow rate at the exit plane, A_e is the nozzle exit area, and V_{exit} is the exit velocity at the nozzle axis.
The specific impulse, I_s, is defined as the thrust per unit weight flow at sea level:

$$I_s = \frac{T}{m^* g_0} \tag{3}$$

Moreover, the thrust coefficient is given by Eq. 4:

$$C_t = \frac{T}{P_0.A_t} \tag{4}$$

where A_t is the throat area and P_0 is the total pressure.

The thrust coefficient and specific impulse are then plotted in Fig. 10. It is clear that thrust is proportional to the mass flow rate from Eq. 2. Hence, the mass

loss through the gaps reduces the thrust and consequently the thrust coefficient. It is also noticed that the slope of C_t line is relatively lower between the conventional nozzle and the nozzle with gap width $0.05D$, whereas it decreases faster when the gap width increases. On the other hand, the specific impulse is, if anything, inversely proportional to the mass flow rate. Therefore, it is seen to increase slightly in the initial stage (gap width of $0.05D$). However, with further increment in gap width, other factors (such as exit pressure and exit velocity) interfere significantly, and the specific impulse decreases.

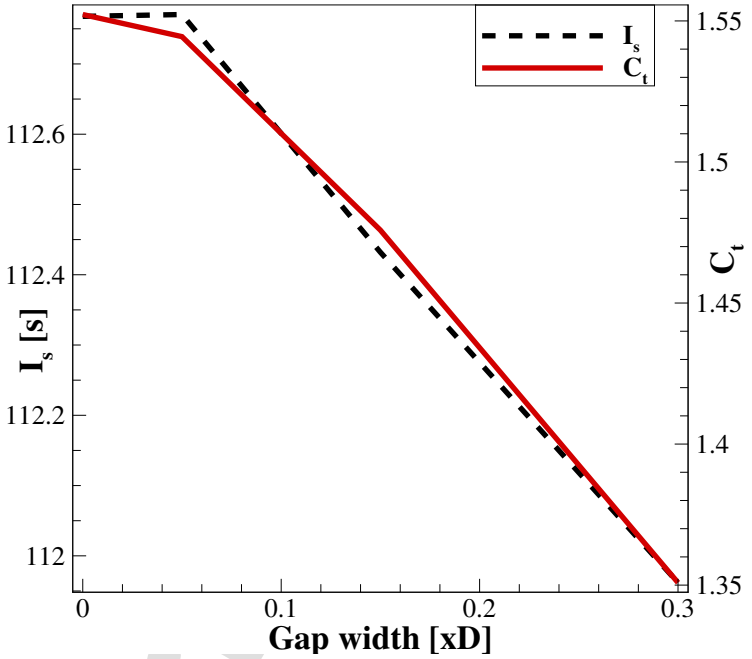

Figure 10: The thrust coefficient and specific impulse for contoured ringed nozzle with different gap width.

3.4. Flow uniformity analysis

As the radially-uniform flow jet is preferable at the outlet of the nozzle for many applications, it becomes of great interest to plot the radial distribution of jet properties at the nozzle exit plane to investigate the role of using the contoured nozzle and subsequently the ringed contoured nozzle. Thus, the radial distribution

of jet density is plotted in Fig. 11a for conical, contoured and ringed nozzles.

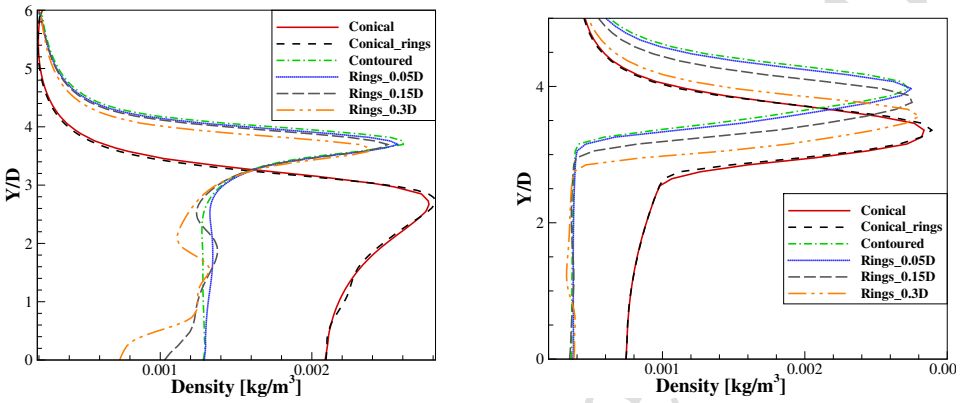

Figure 11: Radial distribution for several nozzles at: (a) Nozzle exit plane and (b) Axial location 15D downstream the exit plane.

It is noticeable from Fig. 11a that the jet resulting from contoured nozzle and the subsequent ringed nozzle is expanded more than the jet resulting from conical and ringed conical nozzles due to the contoured wall shape. It is also seen that the presence of rings creates a disturbance in the radial distribution at the nozzle exit, resulting from the impact of sharp-edged rings, and propagates downstream. However, the variation in distribution is decreased as the gap width is decreased, and the contoured ringed nozzle with a minimum gap width shows a similar trend to the conventional contoured nozzle. Furthermore, in Fig. 11b, the radial distribution of density is plotted at an axial location of 15D downstream of the nozzle exit plane to examine the uniformity and height of the supersonic core after it leaves the nozzle. It can be deduced that the jet maintains its height for the said axial distance and further enhances its radial uniformity as it propagates downstream. Moreover, the conventional nozzle and the ringed nozzle with minimum gap width seems to attain the maximum core height ($3Y/D$), manifesting the improvement in the flow resulting from nozzle shape optimisation. Furthermore, one can notice from Fig. 11a and 11b that the radial distribution in the shear layer area is not regular, i.e., the density starts with a low value outside the jet boundaries, and grows to a large value within the shear layer, then decreases rapidly towards the supersonic core. To probe this phenomenon, other jet parameters such as pressure and temperature have to be studied. Hence, the temperature and pressure

distribution is plotted at the same two locations, viz, at the nozzle exit plane and at an axial location of 15D downstream the exit, Fig. 12 and 13, respectively.

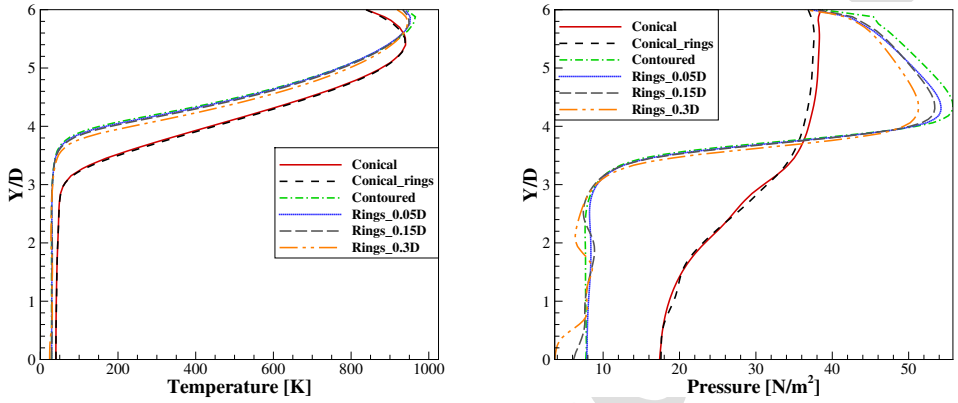

Figure 12: Radial distribution of temperature and pressure at the nozzle exit plane: (a) Temperature and (b) Pressure.

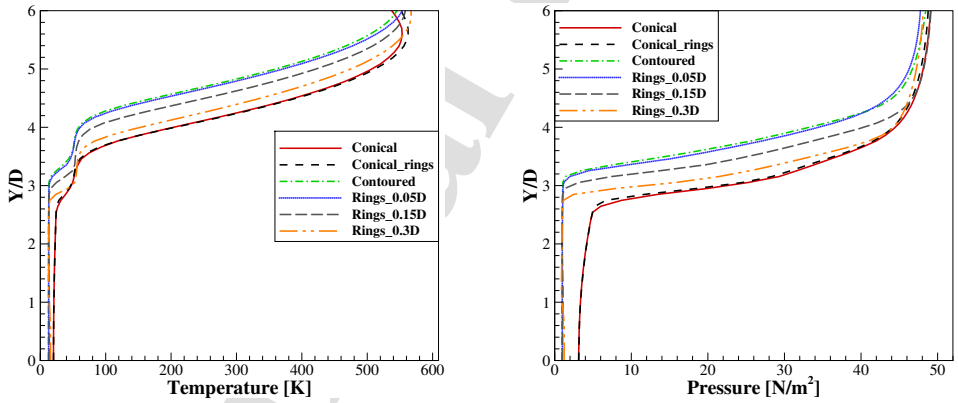

Figure 13: Radial distribution of temperature and pressure at 15D downstream of nozzle exit plane: (a) Temperature and (b) Pressure.

Figures 12 and 13 reveal a regular distribution for the temperature throughout the shear layer. However, the pressure distribution is seen to increase and then decrease across the shear layer, adopting the same trend of density, which justifies

the density distribution. In the case of free supersonic jet, the shear layer is formed from the viscous effects, thus, the shear layer has a rapid variation in density and pressure. That is why the pressure and density are noticed to rapidly increase, and then decrease to match the flow parameters at the supersonic inviscid core. This process causes the irregular radial distribution of density and pressure noticed in Fig. 11, 12 and 13.

Although the ringed nozzles show non-uniformity in the flow field at the nozzle exit and downstream, the ringed nozzle with small gap width, namely 0.05D, shows a matching profile of the conventional contoured nozzle throughout the jet core. Thus, using a ringed nozzle with narrow gaps imitates the performance of a conventional nozzle with minimal mass flow loss and has the ability to compensate the change in back pressure.

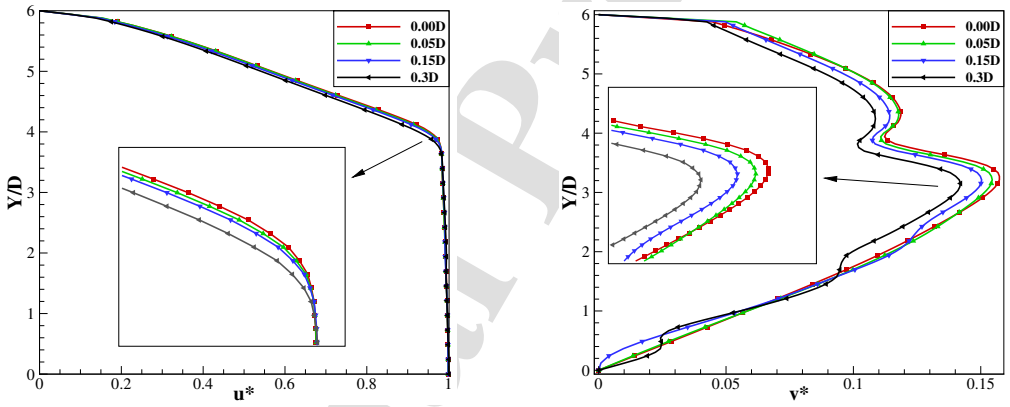

Figure 14: Radial distribution at the nozzle exit for the normalised (a) Axial velocity and (b) Radial velocity.

Since the supersonic jet is desired for different applications that have different preferences regarding the jet, it is of great interest to further examine the jet velocity at the exit. Therefore, the radial distribution of normalised axial and radial velocity at the nozzle exit plane is plotted in Fig. 14 for the conventional nozzle (0.00D) and the ringed nozzles with three gap widths. It is evident here that the nozzle with 0.05D gap width would be the most feasible for the maximum height of inviscid supersonic core. If minor compromise is accepted for the inviscid core height, then better uniformity at the nozzle exit can be seen for the nozzle with

0.3D gap width since it produces the minimum value of radial velocity at exit. Hence, the nozzle gap can be adjusted as per the nozzle requirements. Therefore, although the improvement in flow quality is not remarkable, the ringed nozzle is able to attain the flow uniformity that is achieved by the conventional nozzle.

3.5. Altitude Compensation Effect

The ringed nozzle offers a significant advantage in achieving optimal performance across a range of pressure ratios compared to conventional contoured nozzles. To demonstrate this advantage, a comparison is made between the two nozzle types at a pressure ratio corresponding to the dimensions of the conventional nozzle. The nozzle geometry corresponds to an area ratio of $A/A^* = 144$, resulting in a total pressure ratio of 25800. Schlieren images presented in Fig. 15a reveal that both the conventional contoured nozzle and the ringed nozzle perform similarly under these conditions. The pressure ratio is then reduced to 11500, which corresponds to an area ratio of 88.83. To adjust for the change in operating conditions, six rings are removed from the end of ringed nozzle to achieve the required area ratio, while the conventional nozzle remains unaltered. The number of rings selected for the nozzle design is intended to demonstrate the altitude-compensating effect. As such, removing 2-3 rings is deemed inconsequential to the area ratio since the nozzle's exit is shaped to uniformly direct the flow. Conversely, excising numerous rings would eliminate a substantial portion of the nozzle's contoured segment and transform it into a semi-conical shape. This is due to the fact that the initial part of the diverging section is designed to accommodate most of the expansion process. The performance of both nozzles is evaluated under the new conditions, and the difference in performance is illustrated in the schlieren image shown in Fig. 15b.

The comparison of the ringed nozzle with the conventional nozzle in ideal operating conditions, as presented in Fig. 15a, indicates negligible differences in performance. However, the ringed nozzle exhibits an advantage in adapting to changes in operating conditions. As demonstrated in Fig. 15b, when the pressure ratio decreases, the ringed nozzle is seen to qualitatively adapt for the change in operating condition, and produce a semi-ideally expanded jet. It should be noted that the remaining rings are a portion of the optimised nozzle shape for the initial dimensions, which may require re-optimisation for the new dimensions (the new length is 17.65 *mm*).

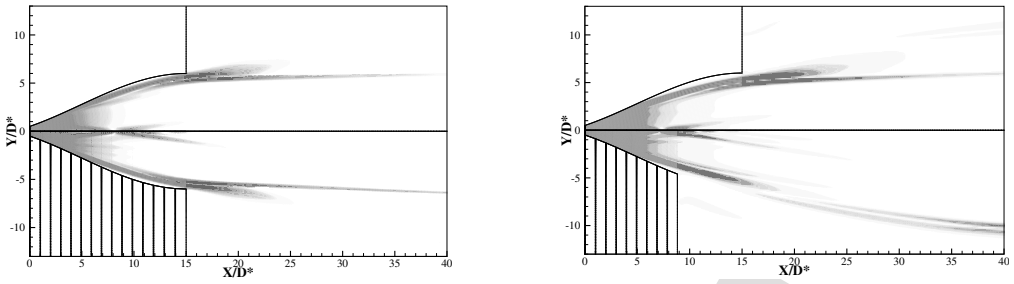

Figure 15: Schlieren images comparing the conventional nozzle and ringed nozzle performance at NPR (a) 25800 and (b) 11500.

To provide more details, the thrust coefficient and specific impulse of the conventional and ringed nozzle are calculated and compared at the two different operating pressure ratios in Fig. 16. This figure shows that the ringed nozzle does not deviate from the performance of conventional nozzle in terms of specific impulse. However, it is seen to perform better in terms of thrust coefficient as it has higher value at low pressure ratio due to the adaptation capability.

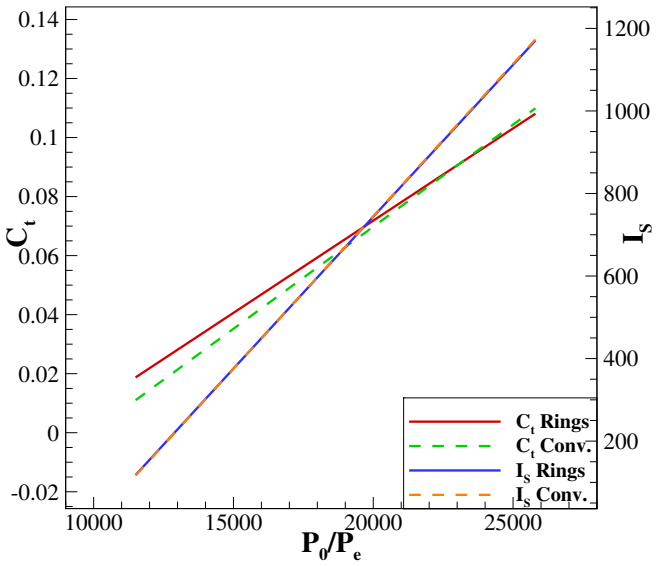

Figure 16: Variation of thrust coefficient and specific impulse for the ringed nozzle and conventional nozzle under two different operating conditions.

4. Conclusion

This work aims to analyse a newly proposed Altitude Compensating Nozzle, the ringed nozzle. It suggests replacing the rigid nozzle wall with a stack of rings, which would benefit the quality of the flow at the nozzle exit and downstream, and account for the changes in the pressure ratio across the nozzle. The conclusion comprises the following findings:

- The ringed nozzle is a viable option for varying operating conditions, as its design maintains the jet properties if the gap width is minimised.
- The gaps between the rings are bleeding slots that remove the low-momentum part of boundary layer, which allows the jet to expand freely and decrease the thickness of shear layer downstream of the nozzle exit plane.
- The ringed nozzle with small gap width imitates the performance and expansion trend of a conventional contoured nozzle and keeps the mass loss, and therefore the energy loss, to the minimum.
- The ringed nozzle is seen to maintain the thrust coefficient and specific impulse when the gap width is kept as minimum.
- When the pressure ratio changes, the ringed nozzle is found to adapt for the change by removing or adding rings from the end to match the exit pressure with the back pressure.
- The specific impulse of the ringed nozzle does not deviate from the performance of a conventional nozzle when the pressure ratio drops. However, the adaptive capability of the ringed nozzle enhances the thrust coefficient under varying conditions. While the ringed nozzle is proven to be a potential solution for altitude-compensating performance, this design needs further experimental validation for actual in-flight performance.

References

[1] K. K. Dingilian, M. Lippe, J. Kubecka, J. Krohn, C. Li, R. Halonen, F. Keshavarz, B. Reischl, T. Kurtén, H. Vehkamaki, et al., New particle formation from the vapor phase: From barrier-controlled nucleation

to the collisional limit, The journal of physical chemistry letters 12 (2021) 4593–4599.

[2] S. Tanimura, Y. Park, A. Amaya, V. Modak, B. E. Wyslouzil, Following heterogeneous nucleation of CO_2 on H_2O ice nanoparticles with microsecond resolution, RSC advances 5 (2015) 105537–105550.

[3] A. Bonnamy, R. Georges, A. Benidar, J. Boissoles, A. Canosa, B. Rowe, Infrared spectroscopy of $(CO_2)_n$ nanoparticles (30< N < 14500) flowing in a uniform supersonic expansion, The Journal of chemical physics 118 (2003) 3612–3621.

[4] Y. Kudryavtsev, R. Ferrer, M. Huyse, P. Van den Bergh, P. Van Duppen, The in-gas-jet laser ion source: Resonance ionization spectroscopy of radioactive atoms in supersonic gas jets, Nuclear Instruments and Methods in Physics Research Section B: Beam Interactions with Materials and Atoms 297 (2013) 7–22.

[5] E. Dudás, N. Suas-David, S. Brahmachary, V. Kulkarni, A. Benidar, S. Kassi, C. Charles, R. Georges, High-temperature hypersonic laval nozzle for $non-LTE$ cavity ringdown spectroscopy, The Journal of chemical physics 152 (2020) 134201.

[6] M. Tizniti, S. D. Le Picard, F. Lique, C. Berteloite, A. Canosa, M. H. Alexander, I. R. Sims, The rate of the $F+H_2$ reaction at very low temperatures, Nature chemistry 6 (2014) 141–145.

[7] L. Biennier, S. Carles, D. Cordier, J.-C. Guillemin, S. D. Le Picard, A. Faure, Low temperature reaction kinetics of $CN^- + HC_3N$ and implications for the growth of anions in titan's atmosphere, Icarus 227 (2014) 123–131.

[8] A. Potapov, A. Canosa, E. Jiménez, B. Rowe, Uniform supersonic chemical reactors: 30 years of astrochemical history and future challenges, Angewandte Chemie International Edition 56 (2017) 8618–8640.

[9] N. A. West, T. J. Millar, M. Van de Sande, E. Rutter, M. A. Blitz, L. Decin, D. E. Heard, Measurements of low temperature rate coefficients for the reaction of CH with CH_2O and application to dark cloud

and *AGB* stellar wind models, The Astrophysical Journal 885 (2019) 134.

[10] N. Suas-David, S. Thawoos, A. Suits, A uniform flow–cavity ring-down spectrometer ($UF-CRDS$): A new setup for spectroscopy and kinetics at low temperature, The Journal of chemical physics 151 (2019) 244202.

[11] A. Canosa, A. Ocaña, M. Antinolo, B. Ballesteros, E. Jiménez, J. Albaladejo, Design and testing of temperature tunable de laval nozzles for applications in gas-phase reaction kinetics, Experiments in Fluids 57 (2016) 1–14.

[12] V. Emelyanov, A. Pustovalov, K. Volkov, Supersonic jet and nozzle flows in uniform-flow and free-vortex aerodynamic windows of gas lasers, Acta Astronautica 163 (2019) 232–243.

[13] S. Yu, B. Yin, Q. Bi, H. Jia, C. Chen, The influence of elliptical and circular orifices on the transverse jet characteristics at supersonic crossflow, Acta Astronautica 185 (2021) 124–131.

[14] H. Kbab, M. Sellam, T. Hamitouche, S. Bergheul, L. Lagab, Design and performance evaluation of a dual bell nozzle, Acta Astronautica 130 (2017) 52–59.

[15] V. Emelyanov, K. Volkov, M. Yakovchuk, Unsteady flow simulation of compressible turbulent flow in dual-bell nozzle with movement of extendible section from its initial to working position, Acta Astronautica 194 (2022) 514–523.

[16] D. Munday, E. Gutmark, J. Liu, K. Kailasanath, Flow structure and acoustics of supersonic jets from conical convergent-divergent nozzles, Physics of Fluids 23 (2011) 116102.

[17] A. K. Perumal, E. Rathakrishnan, Scaling law for supersonic core length in circular and elliptic free jets, Physics of Fluids 33 (2021) 051707.

[18] N. Suas-David, V. Kulkarni, A. Benidar, S. Kassi, R. Georges, Line shape in a free-jet hypersonic expansion investigated by cavity ring-down spectroscopy and computational fluid dynamics, Chemical Physics Letters 659 (2016) 209–215.

[19] G. Rao, Approximation of optimum thrust nozzle contours, ARS J. 30 (1960) 561.

[20] H. Ogawa, R. R. Boyce, Nozzle design optimization for axisymmetric scramjets by using surrogate-assisted evolutionary algorithms, Journal of Propulsion and Power 28 (2012) 1324–1338.

[21] S. Brahmachary, H. Ogawa, Multipoint design optimization of busemann-based intakes for scramjet-powered ascent flight, Journal of Propulsion and Power (2021) 1–18.

[22] S. Brahmachary, G. Natarajan, N. Sahoo, On maximum ballistic coefficient axisymmetric geometries in hypersonic flows, Journal of Spacecraft and Rockets 55 (2017) 518–522.

[23] A. Jraisheh, E. Dudas, N. Suas-David, R. Georges, V. Kulkarni, Low-fidelity approach for contoured nozzle design, Journal of Spacecraft and Rockets (2022) 1–11.

[24] C. Heath, E. J. Nielsen, M. A. Park, J. S. Gray, Aerodynamic shape optimization of a two-stream supersonic plug nozzle, in: 53rd AIAA Aerospace Sciences Meeting, 2015, p. 1047.

[25] D. B. Atkinson, M. A. Smith, Design and characterization of pulsed uniform supersonic expansions for chemical applications, Review of scientific instruments 66 (1995) 4434–4446.

[26] D. Davidenko, Y. Eude, F. Falempin, Numerical study on the annular nozzle optimization for rocket application, in: 16th AIAA/DLR/DGLR International Space Planes and Hypersonic Systems and Technologies Conference, 2009, p. 7390.

[27] A. Mason, H. Broadhurst, Monte carlo modeling of rocket motor multiple nozzle designs, in: 28th Joint Propulsion Conference and Exhibit, 1992, p. 3356.

[28] R. Parsley, K. van Stelle, Altitude compensating nozzle evaluation, in: 28th Joint Propulsion Conference and Exhibit, 1992, p. 3456.

[29] G. Hagemann, H. Immich, T. Van Nguyen, G. E. Dumnov, Advanced rocket nozzles, Journal of Propulsion and Power 14 (1998) 620–634.

[30] M. Horn, S. Fisher, Dual-bell altitude compensating nozzles, NASA CR-194719 (1994) 140–147.

[31] R. Stark, C. Génin, D. Schneider, C. Fromm, Ariane 5 performance optimization using dual-bell nozzle extension, Journal of Spacecraft and Rockets 53 (2016) 743–750.

[32] R. Stark, C. Génin, C. Mader, D. Maier, D. Schneider, M. Wohlhüter, Design of a film cooled dual-bell nozzle, Acta Astronautica 158 (2019) 342–350.

[33] D. S. Jones, T. T. Bui, J. H. Ruf, Proposed flight research of a dual-bell rocket nozzle using the nasa F-15 airplane, in: 49th AIAA/ASME/SAE/ASEE Joint Propulsion Conference, 2013, p. 3954.

[34] D.-S. Ha, H. J. Kim, Dynamic characteristic modeling and simulation of an aerospike-shaped pintle nozzle for variable thrust of a solid rocket motor, Acta Astronautica 201 (2022) 364–375.

[35] G. J. Harloff, G. E. Smith, Supersonic-inlet boundary-layer bleed flow, AIAA journal 34 (1996) 778–785.

[36] W. Wong, The application of boundary layer suction to suppress strong shock-induced separation in supersonic inlets, in: 10th Propulsion Conference, 1974, p. 1063.

[37] B. Willis, D. Davis, W. Hingst, Flow coefficient behavior for boundary layer bleed holes and slots, in: 33rd aerospace sciences meeting and exhibit, 1995, p. 31.

[38] M. Fukuda, E. Reshotko, W. Hingst, Control of shock-wave boundary-layer interactions by bleed in supersonic mixed compression inlets, in: 11th Propulsion Conference, 1975, p. 1182.

[39] A. Weiss, H. Olivier, Influence of boundary layer bleed slot width onto static and total pressure recovery of a shock train, in: 30th International Symposium on Shock Waves 2, Springer, 2017, pp. 1205–1210.

[40] V. Betelin, A. Kushnirenko, N. Smirnov, V. Nikitin, V. Tyurenkova, L. Stamov, Numerical investigations of hybrid rocket engines, Acta Astronautica 144 (2018) 363–370.

[41] A. Kushnirenko, L. Stamov, V. Tyurenkova, M. Smirnova, E. Mikhalchenko, Three-dimensional numerical modeling of a rocket engine with solid fuel, Acta Astronautica 181 (2021) 544–551.

[42] J. Bibin, K. Vinayak, Investigation of energy deposition technique for drag reduction at hypersonic speeds, in: Applied Mechanics and Materials, volume 367, Trans Tech Publ, 2013, pp. 222–227.

[43] B. John, V. Kulkarni, Numerical assessment of correlations for shock wave boundary layer interaction, Computers & Fluids 90 (2014) 42–50.

[44] B. John, V. Kulkarni, Effect of leading edge bluntness on the interaction of ramp induced shock wave with laminar boundary layer at hypersonic speed, Computers & Fluids 96 (2014) 177–190.

[45] B. John, S. Surendranath, G. Natarajan, V. Kulkarni, Analysis of dimensionality effect on shock wave boundary layer interaction in laminar hypersonic flows, International Journal of Heat and Fluid Flow 62 (2016) 375–385.

[46] B. John, V. Kulkarni, Alterations in critical radii of bluntness of shock wave boundary layer interaction, Journal of Aerospace Engineering 30 (2017) 04017022.

[47] N. Smirnov, V. Betelin, R. Shagaliev, V. Nikitin, I. Belyakov, Y. N. Deryuguin, S. Aksenov, D. Korchazhkin, Hydrogen fuel rocket engines simulation using logos code, International Journal of Hydrogen Energy 39 (2014) 10748–10756.

[48] N. Smirnov, V. Betelin, V. Nikitin, L. Stamov, D. Altoukhov, Accumulation of errors in numerical simulations of chemically reacting gas dynamics, Acta Astronautica 117 (2015) 338–355.

[49] Y. Otobe, H. Kashimura, S. Matsuo, T. Setoguchi, H.-D. Kim, Influence of nozzle geometry on the near-field structure of a highly underexpanded sonic jet, Journal of Fluids and Structures 24 (2008) 281–293.

[50] A. Jraisheh, J. Chutia, V. Kulkarni, Alteration in structure of underexpanded freejet through gas-dynamic perspective, AIAA Journal (2021) 1–9.

Highlights

Altitude Compensating Ringed Nozzle

Ali Jraisheh, Jubajyoti Chutia, Abdessamad Benidar, Vinayak Kulkarni

- A novel design of an altitude compensating nozzle by using a stack of parallel rings.
- The performance is not affected when a small gap width between the rings.
- The nozzle is able to perform ideally under varying pressure ratios, without requiring separate nozzle for each pressure ratio.

Declaration of interests

☐ The authors declare that they have no known competing financial interests or personal relationships that could have appeared to influence the work reported in this paper.